



HAL
open science

Comparison of heat transfer performance of water-based graphene nanoplatelet- and multi-walled carbon nanotube-nanofluids in a concentric tube heat exchanger

Sebastian Dayou, Tiew Wei Ting, Brigitte Vigolo

► To cite this version:

Sebastian Dayou, Tiew Wei Ting, Brigitte Vigolo. Comparison of heat transfer performance of water-based graphene nanoplatelet- and multi-walled carbon nanotube-nanofluids in a concentric tube heat exchanger. *Diamond and Related Materials*, 2022, 125, pp.108976. 10.1016/j.diamond.2022.108976 . hal-03792283

HAL Id: hal-03792283

<https://hal.univ-lorraine.fr/hal-03792283>

Submitted on 30 Sep 2022

HAL is a multi-disciplinary open access archive for the deposit and dissemination of scientific research documents, whether they are published or not. The documents may come from teaching and research institutions in France or abroad, or from public or private research centers.

L'archive ouverte pluridisciplinaire **HAL**, est destinée au dépôt et à la diffusion de documents scientifiques de niveau recherche, publiés ou non, émanant des établissements d'enseignement et de recherche français ou étrangers, des laboratoires publics ou privés.

Comparison of heat transfer performance of water-based graphene nanoplatelet- and multi-walled carbon nanotube-nanofluids in a concentric tube heat exchanger

Sebastian Dayou*^a, Ting Tiew Wei^a and Brigitte Vigolo^b

^a School of Engineering and Technology, University College of Technology Sarawak, No. 1, Jalan Universiti, 96000 Sibu, Sarawak, Malaysia

^b Université de Lorraine, CNRS, IJL, F-54000 Nancy, France

Abstract

Carbon nanomaterials are of great interest for next generation nanofluids. Carbon nanotubes and graphene are, in particular, highly thermally conductive and their use as thermal fluid is gaining momentum among the research community. This work investigates the thermal performance of graphene nanoplatelet (GnP)-nanofluid and multi-walled carbon nanotube (MWCNT)-nanofluid by using a concentric pipe heat exchanger. The prepared nanofluid flowed in the inner pipe as hot fluid, which was in the opposite direction of a colder water flow in the annulus pipe. The investigation was conducted by varying the volumetric flow (from 1.5 to 2.5 L/min) and nanofluid concentration (from 0.01 to 0.35 vol.%). The heat transfer coefficient (HTC) of GnP-nanofluid was observed to be superior to that of MWCNT-nanofluid. The maximum increase in HTC relative to the pure base fluid is approximately 16.8, 24.2 and 26.1% for GnP-nanofluid; and 8.8, 13.8 and 14.4 % for MWCNT-nanofluid flowing at 1.5, 2.0 and 2.5 L/min, respectively. This positive impact on heat transfer performance enhancement reached the maximum when an optimum concentration is reached in both nanofluids. Compared to the maximum HTC ratio brought by MWCNT-nanofluid at 0.15 vol.% and 2.5 L/min, GnP-nanofluid produced a greater HTC ratio, even at relatively low concentration (0.05 vol.%) and volumetric flow (1.5 L/min) which is rather desirable for practical applications.

Keywords: *nanofluids; graphene nanoplatelets; multi-walled carbon nanotubes; concentric heat exchanger; heat transfer coefficient*

*Corresponding author. E-mail: sebastian@ucts.edu.my (S. Dayou)

1.0 Introduction

Unveiling the role of heat transfer fluids is key to improve efficiency of heat exchange systems that can be found in automotive radiators, industrial machines, solar photovoltaic systems and many other applications. In recent decades, the utilization of nanofluids as thermal medium has garnered great interest due to their excellent thermal properties. These nanofluids are expected to produce a more efficient heat transfer to meet the growing need for saving energy [1, 2]. Nanofluids are essentially conventional heat transfer fluids which contain solid nanoparticles of high intrinsic thermal conductivity [3]. Such nanofluids are currently considered as the core element of future thermal management technologies.

In the early stage of nanofluid research, the experimental studies focused on the thermal characteristic investigation of metal-oxide and metal nanofluids [3-6] and then expanded to carbon-based nanofluids [7, 8]. Compared to metal-oxide and metal nanoparticle, carbon-based nanofluids, *i.e.* graphene and carbon nanotube (CNT) are more attractive in view of their high-thermal-conductivity characteristics [9]. Furthermore, they can produce heat transfer enhancement at a relatively smaller content due to their lower density and high aspect ratio [10]. This makes these carbon-based nanofluids a much better alternative than their metal-based counterpart for practical applications since their lower concentration level will produce a lower level of viscosity and, in turn, produce a rather smooth flow and a relatively low pumping requirement in the heat exchange system [11, 12].

Numerous experimental works have been performed to scrutinize the performance of CNTs or graphene suspended in various kinds of thermal exchangers [2, 8]. However, a direct comparison between these two types of carbon nanofluids under the same operating conditions and the same exchanger remains scarce. External comparison among published works in literature is complicated because of the relatively high number of parameters which also depend on the large variety of nanofluid systems prepared with different types of base fluid, different procedures for nanofluid preparation, different nanoparticle concentration ranges, with or without surfactants which can also be of several natures, among others. Moreover, the used

heat exchanger geometry is expected to strongly impact the outcomes. To establish this comparison is important, especially to provide levers to develop high thermal performance nanofluids. In this study, the thermal performances of aqueous GnP- and MWCNT-nanofluids in a concentric pipe heat exchanger are compared. As far as we know, this is the first time such comparison is made using this type of heat exchanger.

2.0 Experimental

2.1 Materials and preparation of nanofluid

GnPs used in this work were obtained from XG Science, Inc., Michigan, USA. They are Grade M GnPs with average particle diameter, thickness and specific surface area of about 25 μm , 6 – 8 nm and 120 – 150 m^2/g , respectively. MWCNTs have an outer diameter, inner diameter, length and specific surface area of 20 – 30 nm, 5 – 10 nm, 10 – 30 μm and at least 110 m^2/g , respectively. They were provided by US Research Nanomaterials, Inc., Texas, USA. The morphologies of these nanoparticles were verified under electron microscopy observations using Hitachi SU8010 FESEM and FEI Tecnai G2 20 S-TWIN HRTEM. These nanoparticles were suspended in 2 liters of distilled water by a high shear homogenizer (DAIHAN HG-15A) comprising of a rotor and a stator used at a rotation of 25000 rpm for 1 h. Nanofluid with volumetric concentrations of 0.01, 0.05, 0.15, 0.25 and 0.35 % were prepared for both GnP and MWCNT nanofluids for the experiments.

2.2 Experimental setup and heat transfer coefficient measurements

The measurements of heat transfer coefficient (HTC) were carried out immediately after the preparation of nanofluid using the Armfield HT31 Tubular Heat Exchanger. The schematic layout of the present heat exchanger unit is illustrated in Fig. 1. The test section consisted of U-shaped concentric pipe of 660 mm in length. The stainless steel inner pipe and the acrylic annulus pipe had outer diameter of 9.5 mm and 12 mm, and wall thickness of 0.6 mm and 3.0 mm, respectively. For HTC measurements, the cold water flowed

from an external water supply with a temperature of 27 °C through the annulus pipe constantly at 1.0 L/min. Meanwhile, the hot fluid (*i.e.* nanofluid) flowed in the inner pipe in counter-flow direction and at varying rates of 1.5, 2.0 and 2.5 L/min. A 2 kW heater was used to heat the nanofluid at 50 °C, which was set as the inlet temperature for the entire tests. The nanofluid were pumped from the hot fluid vessel to the test section, then back into the vessel and continuously circulating in the same loop throughout the test. There were six type-K thermocouples installed at fixed locations and connected to a data logger to measure the temperatures at inlet, middle and outlet of both hot and cold fluid streams. To avoid fouling effect and ensuring the reproducibility of experimental data of the prepared nanofluids, the inner tube was cleaned by circulating 2 % solution of Decon 90 with water in between experiment runs to remove any deposit that may have formed on the surface wall. After cleaning, the inner pipe was flushed with water at a speed of 8 L/min for several minutes and was repeated thrice. Prior to every experimental run, a preliminary experiment using distilled water as the hot fluid was carried out to ensure data reproducibility.

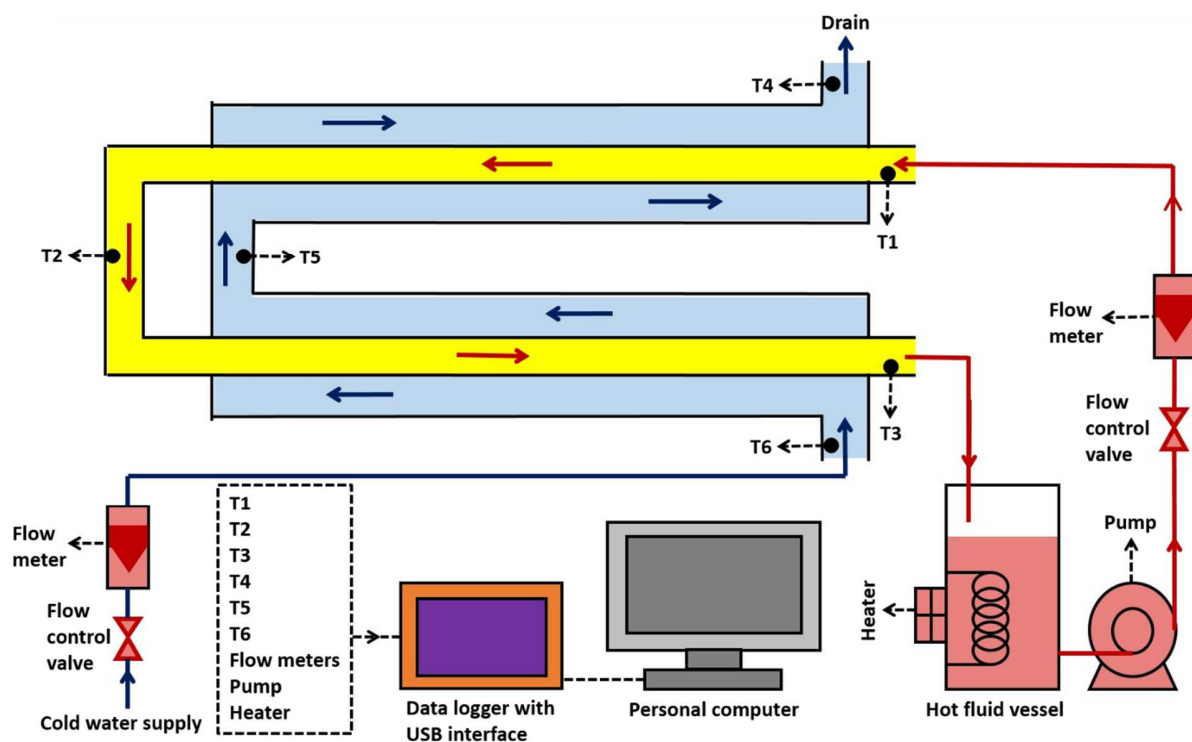


Fig. 1 Schematic layout of the heat exchanger unit

2.3 Data calculation

Nanofluid thermal conductivity (k_{nf}) can be obtained by using the correlation that considers the nanoparticle shape effect as proposed by Hamilton and Crosser [13] as follows:

$$\frac{k_{nf}}{k_{bf}} = \frac{k_{np} + (n-1)k_{bf} - (n-1)\phi(k_{bf} - k_{np})}{k_{np} + (n-1)k_{bf} + \phi(k_{bf} - k_{np})} \quad (1)$$

where k_{np} is nanoparticle thermal conductivity, k_{bf} represents the base fluid thermal conductivity, ϕ is nanoparticle volume fraction and n is an empirical shape factor as defined by:

$$n = \frac{3}{\psi} \quad (2)$$

where ψ refers to sphericity which can be expressed as:

$$\psi = \frac{\pi^{\frac{1}{3}}(6v_{np})^{\frac{2}{3}}}{A_{np}} \quad (3)$$

where v_{np} and A_{np} is the volume and surface area of the nanoparticles, respectively. Maron and Pierce model [14] can be employed to predict the nanofluid viscosity, μ_{nf} :

$$\frac{\mu_{nf}}{\mu_{bf}} = \left(1 - \frac{\phi}{\phi_m}\right)^{-2} \quad (4)$$

where μ_{bf} is base fluid viscosity. This viscosity correlation takes into account the nanoparticle aspect ratio, r (*i.e.* shape) from the maximum packing fraction, ϕ_m , as derived by Mueller *et al.* [15] given below:

$$\phi_m = \frac{2}{0.321r + 3.02} \quad (5)$$

HTC which measures the thermal performance of the nanofluids, is estimated by using:

$$U = \frac{Q}{A \times LMTD} \quad (6)$$

where A is heat transmission area, Q is heat transport rate from nanofluid and $LMTD$ is the logarithmic mean temperature difference, which is the temperature driving force of the heat transport in heat exchanger.

Q and $LMTD$ can be determined from:

$$Q = \dot{m}_{nf} \times C_{p,nf}(T_{nf,in} - T_{nf,out}) \quad (7)$$

$$LMTD = \frac{(T_{nf,in} - T_{w,out}) - (T_{nf,in} - T_{w,in})}{\ln\left(\frac{T_{nf,in} - T_{w,out}}{T_{nf,out} - T_{w,in}}\right)} \quad (8)$$

where \dot{m}_{nf} is the mass flow rate of nanofluid, $T_{nf,in}$ and $T_{nf,out}$ represent the nanofluid temperatures at inlet and outlet of inner pipe, while $T_{w,out}$ and $T_{w,in}$ are the water temperature at inlet and outlet in the annulus pipe. As reported by Pak and Cho [16], nanofluid density, ρ_{nf} , can be predicted from:

$$\rho_{nf} = (1 - \phi)\rho_{bf} + \phi\rho_{np} \quad (9)$$

The nanofluid specific heat capacity, $C_{p,nf}$, can be expressed as [17]:

$$C_{p,nf} = \frac{(1 - \phi)(\rho C_p)_{bf} + \phi(\rho C_p)_{np}}{\rho_{nf}} \quad (10)$$

3.0 Results and discussion

Fig. 2 illustrates the images of the used GnPs (Figs. 2a and 2c) and MWCNTs (Figs. 2b and 2d) as observed under FESEM and HRTEM. They ascertain the typical morphology of the crumpled feature of thin GnPs and the fibrous structure of the MWCNTs, respectively. Based on the images of the MWCNTs, it is verified that the outer diameter of MWCNTs are within the range of 20 – 30 nm as stated by the supplier. MWCNTs with larger diameter were also noticed in the sample but in a very small quantity.

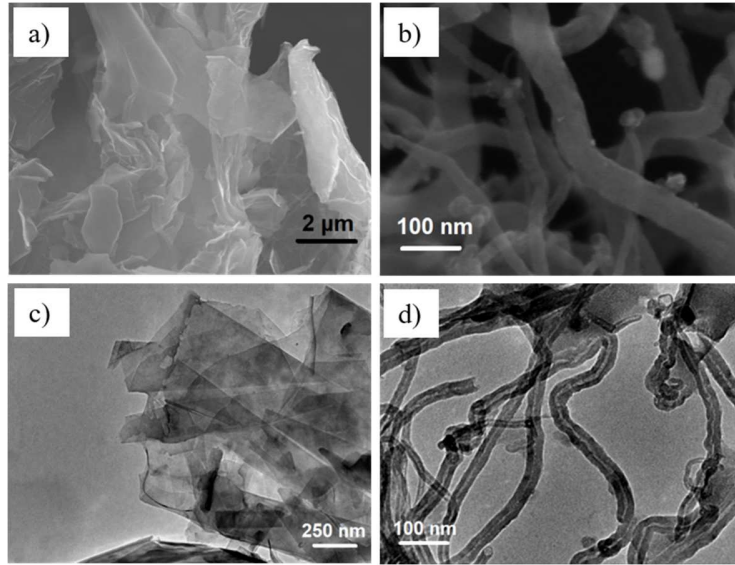


Fig. 2 Typical morphology of the used GnPs (a, c) and MWCNTs (b, d) observed under FESEM and HRTEM, respectively.

Fig. 3 compares the thermal conductivity and viscosity between GnP- and MWCNT-nanofluid by using the correlations given in Eqs. (1) to (5). It is obvious that k_{nf} of GnP-nanofluid is greater than that of MWCNT-nanofluid for all volumetric concentrations. Meanwhile, μ_{nf} of GnP-nanofluid show lower values than that of MWCNT-nanofluid for all the studied concentrations. The difference of k_{nf} and μ_{nf} between both nanofluids becomes significant with increasing concentration. Based on these results, GnP-nanofluids manifest a better thermal medium in view of their higher k_{nf} and lower μ_{nf} as compared to MWCNT-nanofluids.

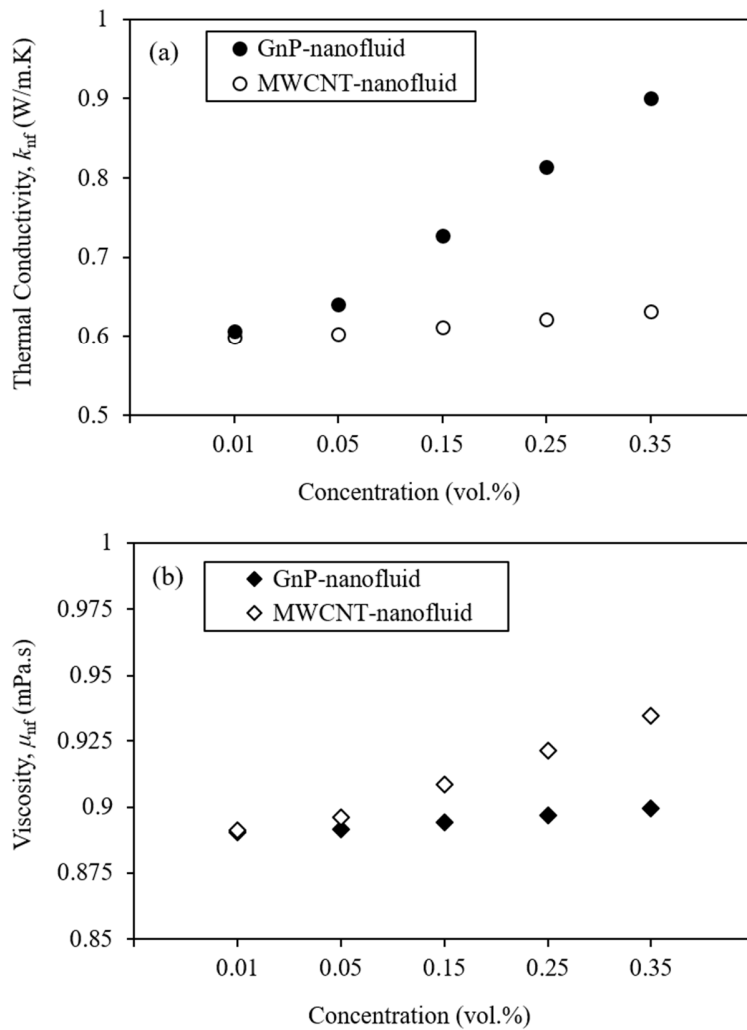


Fig. 3 (a) Thermal conductivity, k_{nf} and (b) viscosity, μ_{nf} of GnP- and MWCNT-nanofluids with different concentrations.

Fig. 4 compares the HTC of GnP-nanofluid, MWCNT-nanofluid and distilled water at varying volumetric concentrations and flow rates. It is observed that the HTC is greatly influenced by the concentration of the nanomaterial used. Both GnP- and MWCNT-nanofluids show the same trend of increasing HTC at the low concentration region and then reducing to a lower HTC at a higher concentration region after a maximum HTC is reached. The maximum increase in HTC relative to the pure base fluid is approximately 16.8, 24.2 and 26.1 % for GnP nanofluid; and 8.8, 13.8 and 14.4 % for MWCNT-nanofluid at 1.5, 2.0 and 2.5 L/min,

respectively. The increase in HTC at the low volumetric concentration up to 0.15 vol.% (0.05 vol.% for 1.5 L/min) is explained by the higher amount of thermally conductive nanoparticles present in the nanofluid as the concentration is increased. The concentration at which the HTC reaches the maximum value shows an optimum concentration. Above this concentration, deterioration in the thermal performances is observed. This shows that the selection of the nanomaterial concentration is of great importance in producing nanofluids with a positive impact on heat transfer performances. This is all the more important because the observed tendency does not follow the commonly agreed behavior regarding the proportionality between thermal performances and nanomaterial concentration in nanofluids. It is indeed widely known that thermal properties of nanofluids are enhanced if the nanoparticle concentration increases [9, 18, 19]. However, with the production cost of nanoparticles being quite high, their concentration has to be optimized in the prepared nanofluids.

As illustrated in Fig. 4, the HTC of the nanofluids is generally greater than that of distilled water. However, when the concentration is the highest at 0.35 vol.%, the HTC of the nanofluid is lower than that of the distilled water at the volumetric flow of 1.5 and 2.0 L/min (for MWCNT-nanofluid). This indicates that when the concentration of suspended nanoparticles is too high, the heat transfer process in the solution deteriorates to a level that is worse than that observed for the base fluid itself. This is often associated with the rise in pressure drop due to high nanofluid viscosity resulted from the high volumetric concentrations of the nanoparticles [11, 16, 20]. This could also explain why the HTC for both MWCNT- and GnP-nanofluids was reduced as the nanofluid concentration is increased after reaching a maximum value at an optimum concentration.

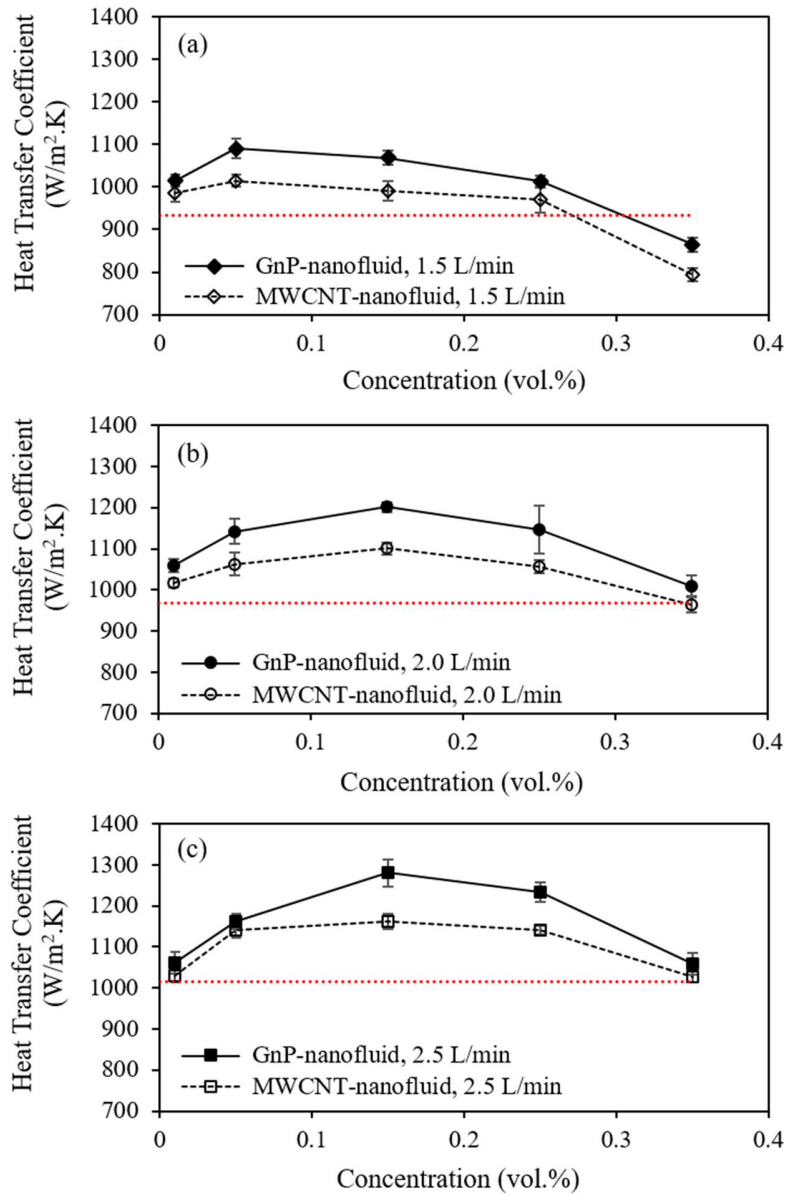


Fig. 4 Variations of HTC with respect to different concentrations of GnP- and MWCNT-nanofluids at volumetric flows of (a) 1.5, (b) 2.0 and (c) 2.5 L/min. The dotted horizontal line is the HTC when distilled water was employed as the hot fluid flow.

Besides, the HTC values are higher when using GnP-nanofluids as compared to those of MWCNT-nanofluids for all concentrations and flow rates. Results in the existing literature have shown that the

intrinsic thermal conductivities of both GnPs and MWCNTs are comparable, where both nanomaterials can reach above 3000 W mK^{-1} [9, 21, 22], but the thermal conduction of the nanofluids containing these nanomaterials can be expected to be different due to their difference in shape, as evidenced by the results shown in Fig. 3a. In particular, the thermal conduction would be superior in a two-dimensional GnP, where phonons can travel in multi-directions parallelly to its surface. In MWCNTs, the travelling of phonons is only limited to one direction which is along the axis of its cylindrical shape.

Generally, the HTC for all the tested fluids is increased at an increasing flow rate. The highest HTC is achieved under the highest volumetric flow of 2.5 L/min at $\phi = 0.15 \text{ vol.}\%$. To further scrutinize the effect of flow rate and nanofluid concentrations on HTC values, a normalized heat transfer coefficient ($U_{\text{nf}}/U_{\text{bf}}$) were plotted against the concentration as depicted in Fig. 5. The figure depicts that for nanofluid at $\phi = 0.15 \text{ vol.}\%$ and above, it is clear that the HTC ratios are the least at the lowest volumetric flow of 1.5 L/min . In contrast, at the lowest concentration of $0.01 \text{ vol.}\%$, the lowest HTC ratio is observed at the highest volumetric flow of 2.5 L/min . These observations are commonly explained by the competing influence between thermal conductivity and formation of thermal boundary layer, where HTC can be roughly expressed as k/δ_t (k = thermal conductivity; δ_t = thermal boundary layer thickness) [23-26]. For a flowing nanofluid, in addition to the nature of thermal conduction of the nanoparticle itself, many scholars had associated the thermal conductivity with multiple nanoparticle-induced interactions in the base fluid *i.e.* Brownian motion, Soret effects, clustering effects, and layering of liquid in molecular level at the liquid-solid interface; these mechanisms could produce a synergistic contribution to k_{nf} [27-29]. The dynamic effects brought by the nanoparticles from these mechanisms can cause a delay or disruption to the flow-induced thermal boundary layer development near the wall surface through the tube length [30]. For instance, existing literature has shown that the suspension of nanoparticles in fluid restricts boundary layer development due to significant migration of nanoparticles when the Brownian motion becomes dominant [31-33]. In this situation, the movement of nanoparticles becomes more chaotic, thus the collisions between

nanoparticles and also with base fluid molecules gets more intense and consequently produces a high energy exchange rate for an augmented HTC [34-37]. Besides, the perceived decline in HTC in both nanofluids above the concentration of 0.15 vol.% could be associated to the favorable development of thermal boundary layer as a result of the rise in viscosity [38, 39]. In this high concentration regime, HTC is generally enhanced with an increasing flow rate. This could be ascribed to the thinning of the thermal boundary layer owing to the intensification of fluid inertial force with an increasing flow rate [37, 40].

For GnP concentration below 0.15 vol.% (below 0.05 vol.% for the MWCNTs), the HTC are greatly affected by the volumetric flow rate. Taking GnP concentration of 0.05 vol.% as an example, HTC is enhanced as the volumetric flow is risen from 1.5 to 2.0 L/min. However, a further increment of the flow rate to 2.5 L/min brings down HTC to a value that is lower than that which is obtained at 1.5 L/min. This shows the existence of a critical volumetric flow rate that could affect HTC values of nanofluid. This is ascribable to the interchange between the competing influence of thermal conductivity and viscosity. At low flow rate, the intensification in thermal conductivity is more significant than viscosity rise, especially since the thermal conductivity could be induced by the effect of nanoparticle dynamics such as the Brownian motion [30, 37]. Increasing the flow rate will further intensify the Brownian motion [30] hence resulting to a further enhancement in thermal conductivity and hence the HTC. This will take effect up to a certain flow rate, beyond which the HTC begins to drop. This reduction in HTC at high flow rate shows that the flow-induced momentum causes hindrance to Brownian motion of nanoparticles and hence adversely influences the heat transfer rate [30, 37].

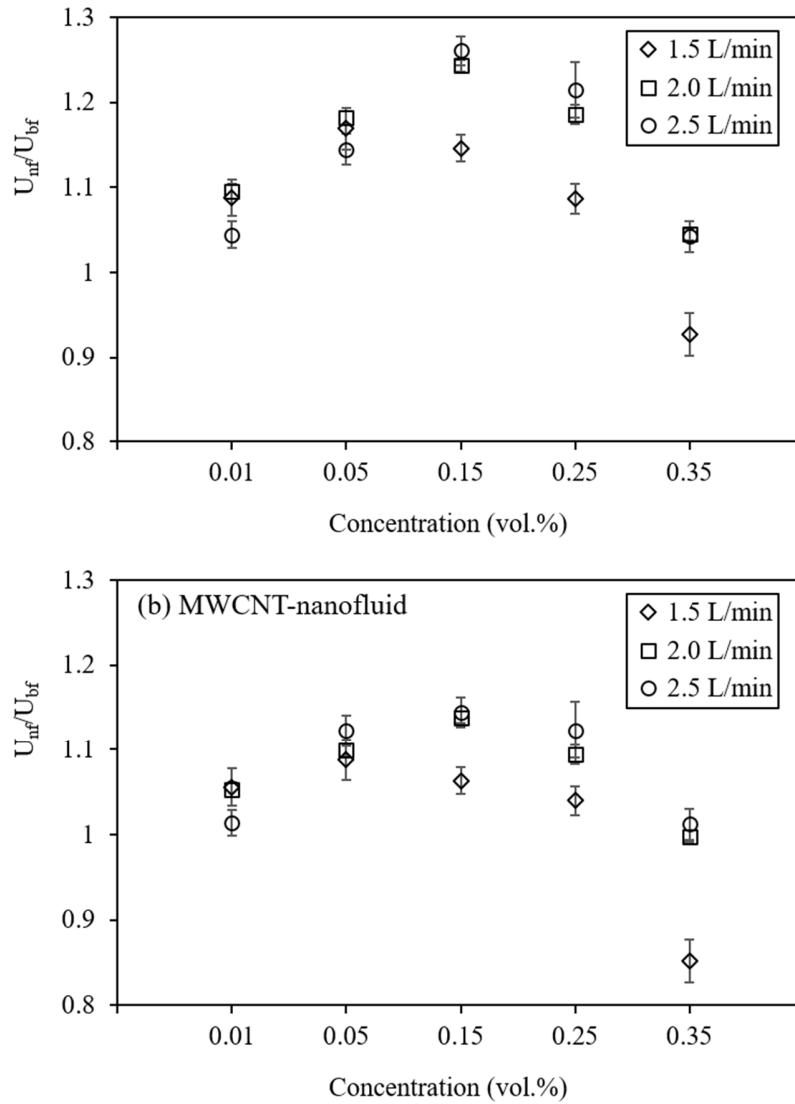


Fig. 5 Variation of HTC ratio of the prepared nanofluids and the used base fluids with respect to nanomaterial concentration in (a) GnP-nanofluids and (b) MWCNT-nanofluids at different volumetric flow rates.

It is worth noting that the maximum HTC ratio brought by MWCNT-nanofluid occurs at a concentration of 0.15 vol.% and at the highest volumetric flow of 2.5 L/min. However, GnP-nanofluid at a lower concentration of 0.05 vol.% produces a higher HTC ratio at the lowest volumetric flow of 1.5 L/min. This implies that GnP can produce a HTC ratio greater than that of MWCNT at even lower concentration and

flow rate, which is more desirable for practical applications. Further examination on the heat transfer rate (Q) revealed that more heat was emitted from the nanofluid when GnP-nanofluid was used as compared to MWCNT-nanofluid at similar concentration as illustrated in Fig. 6. The variation of Q portrays a similar trend with that observed for HTC behavior as shown in Fig. 4a since they are proportional to one another as presented in Eq. (6). Besides, the Q of nanofluids is also proportional to the difference in temperature between the inlet and outlet of the hot section ($T_1 - T_3$) as given in Eq. (7). Hence, the higher Q of GnP-nanofluids when compared to that of MWCNT-nanofluids is caused by a larger temperature difference ($T_1 - T_3$) brought by the former as shown in Fig. 7. From this observation, it is clear that the higher HTC ratio brought by GnP-nanofluids as compared to MWCNT-nanofluids is attributed to their ability to transmit a greater amount of heat. In other work, MWCNT-nanofluids were found to produce higher HTC than observed for GnP-nanofluids in a plate heat exchanger, but no details given regarding the dimension of the GnP and MWCNT nanoparticles that were used [41, 42]. Information on the dimension of nanoparticles is very important since it has huge impact on k_{nf} . For instance, the intrinsic thermal conductivity of GnP can be affected by its number of layers (*i.e.* thickness) [43]. Besides, the intensity of Brownian motion is influenced by the length of MWCNTs where shorter length could move faster and there is a lower probability to entangle with each other [44]. In a nutshell, the discussion given above points out to the important influence of size and shape (*i.e.* aspect ratio) of carbon nanomaterials for heat transfer performance enhancement.

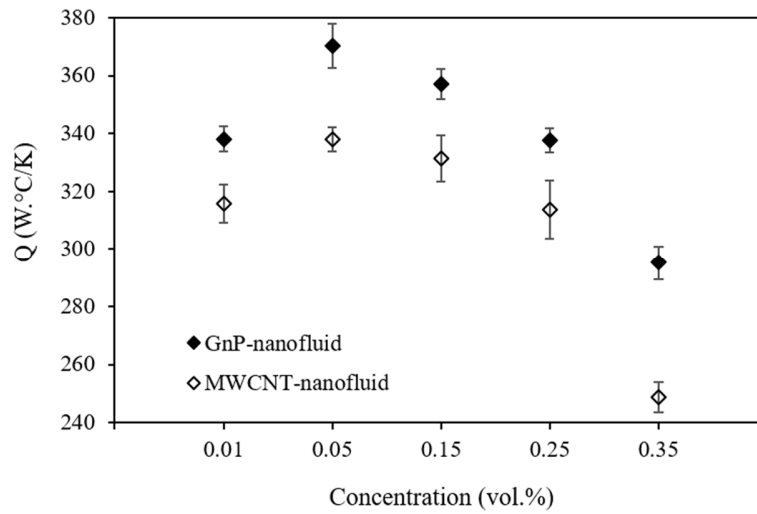


Fig. 6 Heat transfer rate from the hot fluid at different volumetric concentrations of GnP- and MWCNT-nanofluids flowing at 1.5 L/min.

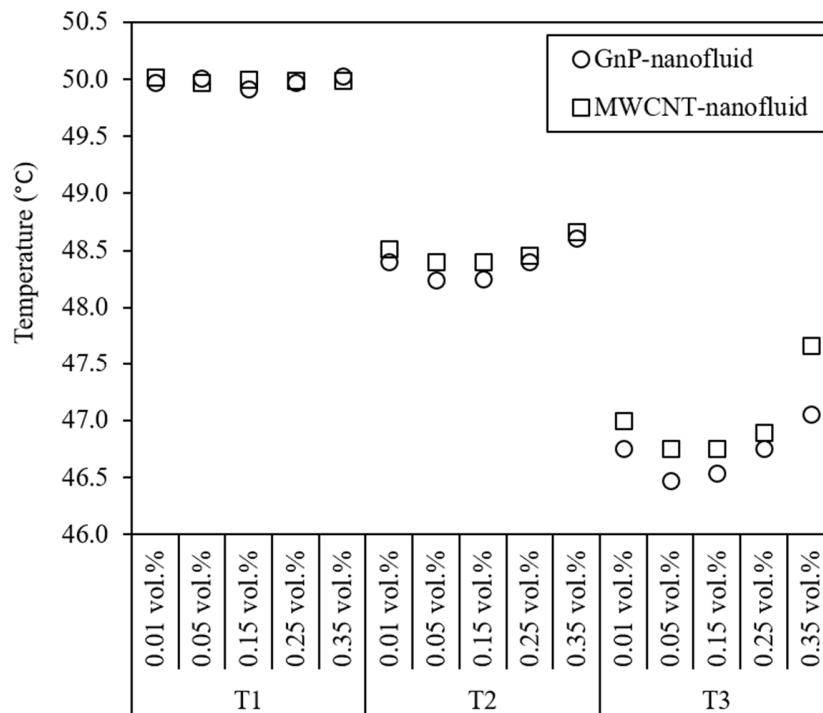


Fig. 7 Temperatures at the inlet (T1), midpoint (T2) and outlet (T3) of the inner tube when different volumetric concentrations of GnP- and MWCNT-nanofluids were flowing at 1.5 L/min.

4.0 Conclusions

In this study, the thermal performance of GnP- and MWCNT-nanofluids are compared by using a concentric tube heat exchanger. GnP-nanofluids are found to produce higher heat transfer coefficient than MWCNT-nanofluid at the respective flow rates and concentrations. The maximum HTC ratio of MWCNT-nanofluid occurs at a concentration of 0.15 vol.% and at the highest volumetric flow of 2.5 L/min. Interestingly, GnP-nanofluids, at a lower concentration of 0.05 vol.% flowing at the lowest volumetric flow of 1.5 L/min, produce a higher HTC ratio, implying that GnPs lead to a greater HTC ratio than that of MWCNTs at an even lower concentration and flow rate. The positive impact of GnPs on the thermal performance enhancement is attributed to its ability to emit a greater amount of heat from the nanofluid. Lastly, this work also points out to the important influence of selecting optimum nanofluid concentration as well as choosing an appropriate size and shape of carbon nanoparticles to enhance the thermal performance of the developed nanofluids.

Acknowledgement

The authors gratefully acknowledge the financial support provided by UCTS Research Grant (1/2018/03).

References

- [1] Eltaweel M, Abdel-Rehim AA (2021) Energy and exergy analysis for stationary solar collectors using nanofluids: A review. *International Journal of Energy Research* 45: 3643-3670. <https://doi.org/10.1002/er.6107>
- [2] Amani M, Amani P, Bahiraei M, et al. (2021) Latest developments in nanofluid flow and heat transfer between parallel surfaces: A critical review. *Advances in Colloid and Interface Science* 294: 102450. <https://doi.org/10.1016/j.cis.2021.102450>
- [3] Choi SUS, Eastman JA (1995) Enhancing thermal conductivity of fluids with nanoparticles, in: *Proceedings of the 1995 ASME International Mechanical Engineering Congress and Exhibition*, ASME, San Francisco, USA. <https://www.osti.gov/biblio/196525>
- [4] Gulzar O, Qayoum A, Gupta R (2021) Experimental study on thermal conductivity of mono and hybrid Al₂O₃-TiO₂ nanofluids for concentrating solar collectors. *International Journal of Energy Research* 45: 4370-4384. <https://doi.org/10.1002/er.6105>

- [5] Issa RJ (2021) A review on thermophysical properties and Nusselt number behavior of Al₂O₃ nanofluids in heat exchangers. *Journal of Thermal Science* 30: 418-431. <https://doi.org/10.1007/s11630-021-1266-1>
- [6] Kumar R, Deshmukh V, Bharj RS (2020) Performance enhancement of photovoltaic modules by nanofluid cooling: A comprehensive review. *International Journal of Energy Research* 44: 6149-6169. <https://doi.org/10.1002/er.5285>
- [7] Barai DP, Bhanvase BA, Sonawane SH (2020) A review on graphene derivatives-based nanofluids: Investigation on properties and heat transfer characteristics. *Industrial & Engineering Chemistry Research* 59: 10231-10277. <https://doi.org/10.1021/acs.iecr.0c00865>
- [8] Ali N, Bahman AM, Aljuwayhel NF, et al. (2021) Carbon-based nanofluids and their advances towards heat transfer applications – A review. *Nanomaterials* 11: 1628. <https://doi.org/10.3390/nano11061628>
- [9] Pavia M, Alajami K, Estellé P, Desforges A, Vigolo B (2021) A critical review on thermal conductivity enhancement of graphene-based nanofluids. *Advances in Colloid and Interface Science* 294: 102452. <https://doi.org/10.1016/j.cis.2021.102452>
- [10] Martínez-Cuenca R, Mondragón R, Hernández L, et al. (2016) Forced-convective heat-transfer coefficient and pressure drop of water-based nanofluids in a horizontal pipe. *Applied Thermal Engineering* 98: 841-849. <https://doi.org/10.1016/j.applthermaleng.2015.11.050>
- [11] Routbort JL, Singh D, Timofeeva EV, Yu W, France DM (2011) Pumping power of nanofluids in a flowing system. *Journal of Nanoparticle Research* 13: 931-937. <https://doi.org/10.1007/s11051-010-0197-7>
- [12] Yazid MNAWM, Sidik NAC, Yahya WJ (2017) Heat and mass transfer characteristics of carbon nanotube nanofluids: A review. *Renewable and Sustainable Energy Reviews* 80: 914-941. <https://doi.org/10.1016/j.rser.2017.05.192>
- [13] Hamilton RL, Crosser OK (1962) Thermal conductivity of heterogeneous two-component systems. *Industrial & Engineering Chemistry Fundamentals* 1: 187-191. <https://doi.org/10.1021/i160003a005>
- [14] Maron SH, Pierce PE (1956) Application of ree-eyring generalized flow theory to suspensions of spherical particles. *Journal of Colloid Science* 11: 80-95. [https://doi.org/10.1016/0095-8522\(56\)90023-X](https://doi.org/10.1016/0095-8522(56)90023-X)
- [15] Mueller S, Llewellyn EW, Mader HM (2010) The rheology of suspensions of solid particles. *Proceedings of the Royal Society A: Mathematical, Physical and Engineering Sciences* 466: 1201-1228. <https://doi.org/10.1098/rspa.2009.0445>
- [16] Pak BC, Cho YI (1998) Hydrodynamic and heat transfer study of dispersed fluids with submicron metallic oxide particles. *Experimental Heat Transfer* 11: 151-170. <https://doi.org/10.1080/08916159808946559>
- [17] Xuan Y, Roetzel W (2000) Conceptions for heat transfer correlation of nanofluids. *International Journal of Heat and Mass Transfer* 43: 3701-3707. [https://doi.org/10.1016/S0017-9310\(99\)00369-5](https://doi.org/10.1016/S0017-9310(99)00369-5)
- [18] Dey D, Kumar P, Samantaray S (2017) A review of nanofluid preparation, stability, and thermo-physical properties. *Heat Transfer—Asian Research* 46: 1413-1442. <https://doi.org/10.1002/htj.21282>
- [19] Ali ARI, Salam B (2020) A review on nanofluid: Preparation, stability, thermophysical properties, heat transfer characteristics and application. *SN Applied Sciences* 2: 1636. <https://doi.org/10.1007/s42452-020-03427-1>

- [20] Williams W, Buongiorno J, Hu L-W (2008) Experimental investigation of turbulent convective heat transfer and pressure loss of alumina/water and zirconia/water nanoparticle colloids (nanofluids) in horizontal tubes. *Journal of Heat Transfer* 130. <https://doi.org/10.1115/1.2818775>
- [21] Kim P, Shi L, Majumdar A, McEuen PL (2001) Thermal transport measurements of individual multiwalled nanotubes. *Physical Review Letters* 87: 215502. <https://doi.org/10.1103/PhysRevLett.87.215502>
- [22] Novoselov KS, Fal'ko VI, Colombo L, et al. (2012) A roadmap for graphene. *Nature* 490: 192-200. <https://doi.org/10.1038/nature11458>
- [23] Aravind SSJ, Baskar P, Baby TT, et al. (2011) Investigation of structural stability, dispersion, viscosity, and conductive heat transfer properties of functionalized carbon nanotube based nanofluids. *The Journal of Physical Chemistry C* 115: 16737-16744. <https://doi.org/10.1021/jp201672p>
- [24] Wang J, Zhu J, Zhang X, Chen Y (2013) Heat transfer and pressure drop of nanofluids containing carbon nanotubes in laminar flows. *Experimental Thermal and Fluid Science* 44: 716-721. <https://doi.org/10.1016/j.expthermflusci.2012.09.013>
- [25] Ding Y, Chen H, He Y, et al. (2007) Forced convective heat transfer of nanofluids. *Advanced Powder Technology* 18: 813-824. <https://doi.org/10.1163/156855207782515021>
- [26] Ding Y, Alias H, Wen D, Williams RA (2006) Heat transfer of aqueous suspensions of carbon nanotubes (CNT nanofluids). *International Journal of Heat and Mass Transfer* 49: 240-250. <https://doi.org/10.1016/j.ijheatmasstransfer.2005.07.009>
- [27] Godson L, Raja B, Mohan Lal D, Wongwises S (2010) Enhancement of heat transfer using nanofluids—An overview. *Renewable and Sustainable Energy Reviews* 14: 629-641. <https://doi.org/10.1016/j.rser.2009.10.004>
- [28] Keblinski P, Phillpot SR, Choi SUS, Eastman JA (2002) Mechanisms of heat flow in suspensions of nano-sized particles (nanofluids). *International Journal of Heat and Mass Transfer* 45: 855-863. [https://doi.org/10.1016/S0017-9310\(01\)00175-2](https://doi.org/10.1016/S0017-9310(01)00175-2)
- [29] Ganvir RB, Walke PV, Kriplani VM (2017) Heat transfer characteristics in nanofluid—A review. *Renewable and Sustainable Energy Reviews* 75: 451-460. <https://doi.org/10.1016/j.rser.2016.11.010>
- [30] Sajid MU, Ali HM (2019) Recent advances in application of nanofluids in heat transfer devices: A critical review. *Renewable and Sustainable Energy Reviews* 103: 556-592. <https://doi.org/10.1016/j.rser.2018.12.057>
- [31] Kumaresan V, Mohaideen Abdul Khader S, Karthikeyan S, Velraj R (2013) Convective heat transfer characteristics of CNT nanofluids in a tubular heat exchanger of various lengths for energy efficient cooling/heating system. *International Journal of Heat and Mass Transfer* 60: 413-421. <https://doi.org/10.1016/j.ijheatmasstransfer.2013.01.021>
- [32] Bahiraei M (2016) Particle migration in nanofluids: A critical review. *International Journal of Thermal Sciences* 109: 90-113. <https://doi.org/10.1016/j.ijthermalsci.2016.05.033>
- [33] Kim D, Kwon Y, Cho Y, et al. (2009) Convective heat transfer characteristics of nanofluids under laminar and turbulent flow conditions. *Current Applied Physics* 9: e119-e123. <https://doi.org/10.1016/j.cap.2008.12.047>
- [34] Abreu B, Lamas B, Fonseca A, Martins N, Oliveira MSA (2014) Experimental characterization of convective heat transfer with MWCNT based nanofluids under laminar flow conditions. *Heat and Mass Transfer* 50: 65-74. <https://doi.org/10.1007/s00231-013-1226-8>
- [35] Wen D, Ding Y (2004) Experimental investigation into convective heat transfer of nanofluids at the entrance region under laminar flow conditions. *International Journal of Heat and Mass Transfer* 47: 5181-5188. <https://doi.org/10.1016/j.ijheatmasstransfer.2004.07.012>

- [36] Xuan Y, Li Q (2003) Investigation on convective heat transfer and flow features of nanofluids. *Journal of Heat Transfer* 125: 151-155. <https://doi.org/10.1115/1.1532008>
- [37] Ahmed M, Eslamian M (2015) Laminar forced convection of a nanofluid in a microchannel: Effect of flow inertia and external forces on heat transfer and fluid flow characteristics. *Applied Thermal Engineering* 78: 326-338. <https://doi.org/10.1016/j.applthermaleng.2014.12.069>
- [38] Duangthongsuk W, Wongwises S (2010) An experimental study on the heat transfer performance and pressure drop of TiO₂-water nanofluids flowing under a turbulent flow regime. *International Journal of Heat and Mass Transfer* 53: 334-344. <https://doi.org/10.1016/j.ijheatmasstransfer.2009.09.024>
- [39] Tiwari AK, Ghosh P, Sarkar J (2013) Performance comparison of the plate heat exchanger using different nanofluids. *Experimental Thermal and Fluid Science* 49: 141-151. <https://doi.org/10.1016/j.expthermflusci.2013.04.012>
- [40] Safaei MR, Ahmadi G, Goodarzi MS, Kamyar A, Kazi SN (2016) Boundary layer flow and heat transfer of FMWCNT/water nanofluids over a flat plate. *Fluids* 1: 31. <https://doi.org/10.3390/fluids1040031>
- [41] Kumar V, Tiwari AK, Ghosh SK (2016) Effect of variable spacing on performance of plate heat exchanger using nanofluids. *Energy* 114: 1107-1119. <https://doi.org/10.1016/j.energy.2016.08.091>
- [42] Warzoha RJ, Fleischer AS (2014) Effect of graphene layer thickness and mechanical compliance on interfacial heat flow and thermal conduction in solid-liquid phase change materials. *ACS Applied Materials & Interfaces* 6: 12868-12876. <https://doi.org/10.1021/am502819q>
- [43] Yan Z, Nika DL, Balandin AA (2015) Thermal properties of graphene and few-layer graphene: applications in electronics. *IET Circuits, Devices & Systems* 9: 4-12. <https://doi.org/10.1049/iet-cds.2014.0093>
- [44] Li F-C, Yang J-C, Zhou W-W, et al. (2013) Experimental study on the characteristics of thermal conductivity and shear viscosity of viscoelastic-fluid-based nanofluids containing multiwalled carbon nanotubes. *Thermochimica Acta* 556: 47-53. <https://doi.org/10.1016/j.tca.2013.01.023>